Ultrahigh birefringence index-guiding photonic crystal fiber and its application for pressure and temperature discrimination

Zhengyong Liu,[1] Chuang Wu,[1,2] Ming-Leung Vincent Tse,[1] Chao Lu,[3] and Hwa-Yaw Tam[1,*]

[1]*Photonics Research Center, Department of Electrical Engineering, The Hong Kong Polytechnic University, Hung Hom, Kowloon, Hong Kong, China*

[2]*Institute of Photonics Technology, Jinan University, Guangzhou 510632, China*

[3]*Photonics Research Center, Department of Electronic and Information Engineering, The Hong Kong Polytechnic University, Hung Hom, Kowloon, Hong Kong, China*

**Corresponding author: hwa-yaw.tam@polyu.edu.hk*

Received February 8, 2013; revised March 24, 2013; accepted March 24, 2013; posted March 25, 2013 (Doc. ID 185106); published April 19, 2013

In this Letter, we reported on an ultrahigh birefringence photonic crystal fiber (PCF) with a germanium-doped elliptical core, which is fabricated in our lab using the stack-and-draw method. An ultrahigh birefringence of 1.1×10^{-2} is obtained experimentally, which is close to the theoretical value of 1.4×10^{-2} at the wavelength of 1550 nm. To our knowledge, this is the highest birefringence reported to date for fabricated index-guiding PCF. Fiber Bragg gratings (FBG) were written in the fiber to confirm its ultrahigh birefringence, and we demonstrated the capability to simultaneously measure the FBG's pressure and temperature experimentally. Because of the large separation of the two FBG peaks (>12 nm), such fiber is a promising candidate for a single polarization device.

OCIS codes: (060.2280) Fiber design and fabrication; (060.2420) Fibers, polarization-maintaining; (060.5295) Photonic crystal fibers; (280.5475) Pressure measurement.

http://dx.doi.org/10.1364/OL.38.001385

Photonic crystal fibers (PCFs) have been attracting great interest in the research community since the first endless single-mode PCF was reported [1], opening a bright future for the design and application of optical fibers. Classified by different light guidance principles, two kinds of PCFs (i.e., index-guiding PCF and photonic bandgap PCF) were mainly investigated to conduct novel applications in optical communications and sensing for transmission, fiber lasers and amplifiers, nonlinear and birefringent devices, and interferometers [2]. To realize a single polarization device and eliminate the polarization mode dispersion, polarization-maintaining fibers (PMFs) with high birefringence (Hi-Bi) are needed. Owing to the flexibility of structure and the feasibility of fabrication, PCF can be made to have Hi-Bi with asymmetric design [3,4] and an elliptical core [5]. PCF technology is far more superior in producing PMFs. Hi-Bi can be achieved simply by introducing two large air holes close to the core of conventional, single-mode PCF [6,7].

Most PMFs exhibit birefringence on the order of 10^{-4} to 10^{-3}. For commonly used PM-1550–01 fiber, (probably the only commercially PM–PCF available from NKT Photonics), the birefringence is $\sim 3.9 \times 10^{-4}$ [8]. Recently, Frazão reported a fiber optic interferometric torsion sensor using a PM–PCF with two large air holes fabricated in an XLIM laboratory, demonstrating a group birefringence of $\sim 8.1 \times 10^{-3}$ [7]. Different asymmetrical PCF structures also were tailored to enhance its birefringence for conduct strain [9] and temperature-independent measurement [10]. The highest experimental birefringences reported for index-guiding PCFs were on the order of 10^{-3} [3,7,11–13]. It should be noted that the highest group birefringence reported were found in a photonic bandgap fiber (0.025 at the wavelength of 1550 nm), achieved via elliptical air core [14,15]. However, this fiber does not allow the inscription of fiber gratings in its core.

In this Letter, we continue from our previous study of Hi-Bi Ge-doped index-guiding PCF [16] to report on an ultrahigh birefringence index-guiding PCF with two large holes and a measured phase modal birefringence of $\sim 1.1 \times 10^{-2}$. To our knowledge, this is the highest value for any microstructured fibers reported to date, and more than an order of magnitude higher than any solid core fibers previously demonstrated. The phase modal birefringence was measured by inscribing FBG in the Ge-doped core, resulting in two distinct Bragg peaks separated by more than 12 nm. The experimental value of birefringence also was confirmed by simulation, which gives a phase modal birefringence of 1.4×10^{-2}. The fiber gave good discrimination in multiparameter measurement. Simultaneous measurement of pressure and temperature using the fiber was conducted.

The Hi-Bi PCF was fabricated in-house using the stack-and-draw technique on a fiber drawing tower (Nextrom OFC20). The fabrication process illustrated in Fig. 1 is similar to the fabrication method we

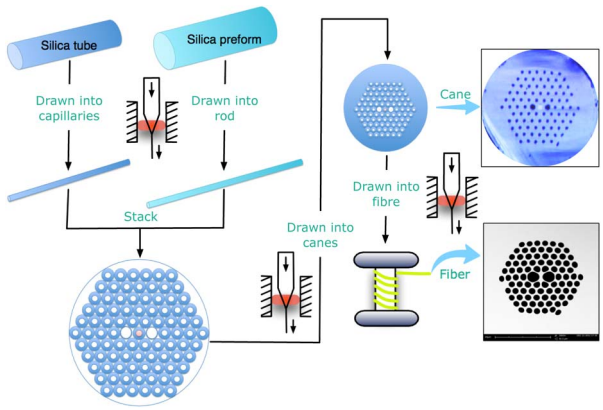

Fig. 1. Schematic diagram of the fabrication of Hi-Bi PCF.

conducted previously for a twin-core PCF [17]. Capillaries with diameter of 1.6 mm were first drawn from a silica tube that has an outer diameter of 44 mm and inner diameter of 17.6 mm. The air fraction was assumed unchanged during drawing. Meanwhile, pure silica rods with different diameters were drawn for stacking. During stacking, a germanium-doped (Ge-doped) rod (1 mm in diameter) was used to replace the center capillary and will eventually become the core of the Hi-Bi PCF. Two large capillaries, with a diameter of 1.6 mm and air fraction of 0.76, were inserted adjacent to the core. The stacked preform was then drawn into canes with a diameter of 1.6 mm. One cane was chosen and inserted into a jacket tube of 7 mm in diameter, which was stretched from a silica tube with inner and outer diameters of 4 and 12 mm, respectively. This ensemble was then drawn into fiber at the temperature of 1870°C. Lower temperature and vacuum control were used to enlarge the air holes, especially the two big holes so that an elliptical core can be formed to obtain Hi-Bi.

Figure 2(a) shows the SEM photo of the cross section of the fabricated Hi-Bi PCF, with x denoting the fast axis and y denoting the slow axis. The outer diameter of the fiber is ~125 μm. The small holes have a diameter of ~2.35 μm and pitch of ~3.04 μm. The two holes adjacent to the core were enlarged with size of 4.3 μm × 3.81 μm. Consequently, the core became elliptical and has a dimension of ~3 μm × 1 μm. The measured propagation loss of the PCF is ~0.2 dB/m. The splicing loss with SMF28 is ~2.1 dB using a technique similar to that used in [17,18], which is in accordance with the value in [19]. Note that two air holes at the outer ring are missing, because two capillaries were broken during stacking. Because they are in the outermost ring, though, the influence of this defect is very small. Simulation of the Hi-Bi PCF was performed using commercial software COMSOL. The refractive index for the core is set as 1.47 and 1.444 for the silica. Two polarized fundamental modes were found, corresponding to LP_{01-x} and LP_{01-y}. The effective refractive indexes for the fast and slow axis are 1.370937 and 1.384772, respectively, showing a phase birefringence (Δn) of 1.4×10^{-2} at the wavelength of 1550 nm. Figures 2(b) and 2(c) illustrates the intensity profile of LP_{01-x} and LP_{01-y}. The ellipticity of modal field is then calculated as ~2.18 from Figs. 2(b) and 2(c).

The Hi-Bi PCF has a Ge-doped core and FBG was inscribed in the core using the phase-mask technique to measure the fiber's birefringence. Two phase masks were used separately in two measurements with pitches of

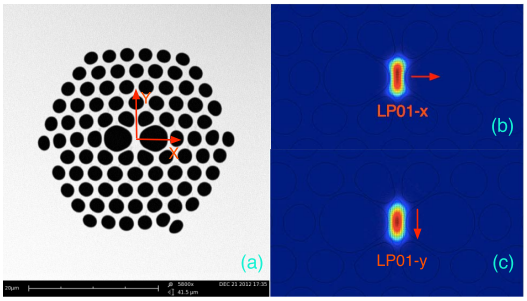

Fig. 2. (a) SEM photo of the section structure of Hi-Bi PCF and the simulated intensity profile of (b) LP_{01-x} and (c) LP_{01-y}.

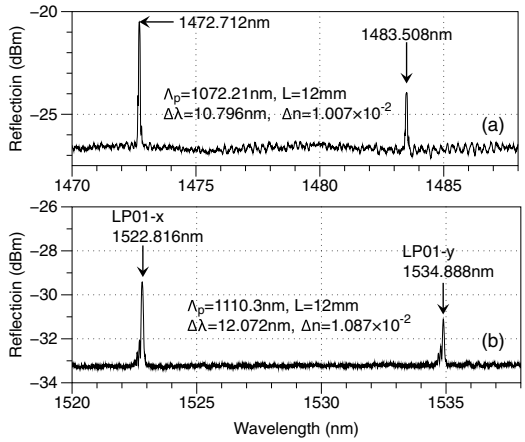

Fig. 3. Reflection spectrum of FBG written in Hi-Bi PCF using phase masks with pitch of (a) 1072.21 nm and (b) 1110.3 nm.

1072.21 and 1110.3 nm. A KrF laser with a wavelength of 193 nm and a 2 mm beam width was used to scan along the fiber for 10 mm. The pulse energy and pulse rate of the laser were 110 mJ and 15 Hz. Figure 3 shows the reflection spectra of the FBGs written on the fiber. The two reflective peaks, corresponding to LP_{01-x} and LP_{01-y} are separated by more than 12 nm, much larger than that of FBG inscribed in commercial PM–PCF (<1 nm) [8]. The large peak separation indicates ultrahigh birefringence of 1.1×10^{-2}, which is close to the simulation value.

The unusually large separation of the two polarized modes permits more accurate measurement of the wavelength shift of the two peaks in the FBG reflection spectrum. FBG written in the Hi-Bi PCF could be used to measure pressure and temperature simultaneously. Since the fiber has an elliptical core and an asymmetrical hole structure, the responses to ambient pressure for the fast and slow axis are different with higher sensitivity for the slow axis [8]. However, the difference between the peaks responding to temperature for both polarizations is very small because both axes exhibit similar thermal expansion. Note that pressure measurement based on birefringence of PM–PCF also was demonstrated, in the form of Sagnac loop interferometer [6] and a modal interferometer [19].

When subjected to pressure and temperature, the wavelength shift for each peak can be expressed as

$$\begin{aligned} \Delta\lambda_x &= S_{x,p} \cdot \Delta P + S_{x,T} \cdot \Delta T, \\ \Delta\lambda_y &= S_{y,p} \cdot \Delta P + S_{y,T} \cdot \Delta T, \end{aligned} \tag{1}$$

where the $S_{x,p}$, $S_{x,T}$, $S_{y,p}$, and $S_{y,T}$ are the sensitivity of pressure and temperature for x- and y-polarized FBG peaks, respectively. Therefore, through simple algebraic conversion, the discrimination between pressure and temperature can be derived as

$$\begin{bmatrix} \Delta T \\ \Delta P \end{bmatrix} = \frac{1}{D} \begin{bmatrix} S_{x,p} & -S_{y,p} \\ -S_{x,T} & S_{y,T} \end{bmatrix} \cdot \begin{bmatrix} \Delta\lambda_y \\ \Delta\lambda_x \end{bmatrix}, \tag{2}$$

where $D = S_{x,p} \cdot S_{y,T} - S_{x,T} \cdot S_{y,p}$.

In our experiments, the FBG was placed inside a pressure chamber to measure hydrostatic pressure.

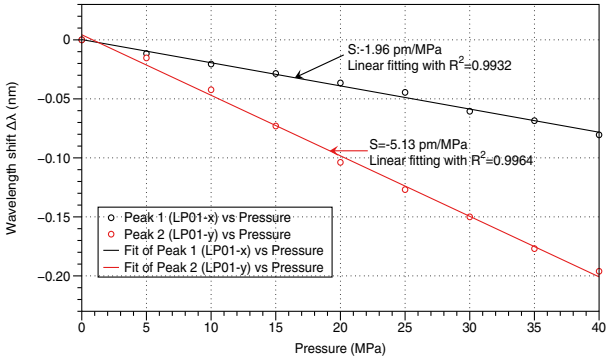

Fig. 4. Wavelength shift for the LP_{01-x} and LP_{01-y} peaks as a function of pressure.

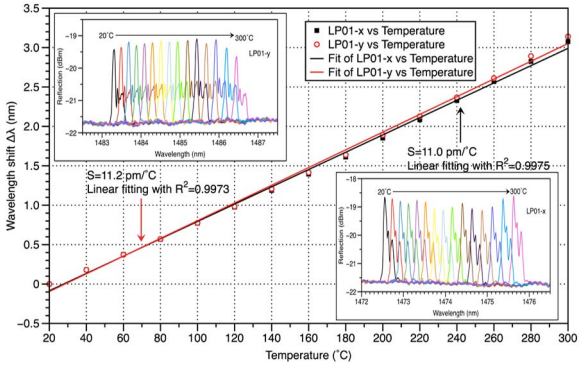

Fig. 5. Wavelength shift for LP_{01-x} peak (black) and LP_{01-y} peak (red) as a function of temperature. Insets show the spectrum shift for both peaks.

The pressure was increased in steps of 5 MPa. As expected, the pressure response for the slow axis was greater than that of the fast axis. Figure 4 shows the wavelength shift for both peaks as a function of hydrostatic pressure from 0 to 40 MPa. From the result, the measured sensitivity for the fast axis is −1.96 pm/MPa and −5.13 pm/MPa for the slow axis, with a good linear-fits, $R^2 = 0.99$.

Temperature measurement was conducted on the same FBG in an oven that was heated from 20°C to 300°C. Figure 5 shows the result of wavelength shift versus temperature. A sensitivity of 11 pm/°C and 11.2 pm/°C was obtained for the fast and slow axis, respectively. The temperature response for both polarizations is very similar (difference <2%), whereas the pressure response of the two peaks has a large difference of 62%. Substitution of the measured sensitivities in Eq. (2) yields

$$\begin{bmatrix} \Delta T \\ \Delta P \end{bmatrix} = \frac{1}{34.48} \begin{bmatrix} -1.96 & 5.13 \\ -11.0 & 11.2 \end{bmatrix} \cdot \begin{bmatrix} \Delta\lambda_y \\ \Delta\lambda_x \end{bmatrix}. \quad (3)$$

Pressure and temperature applied to the FBG inscribed in the Hi-Bi PCF can be determined simultaneously using Eq. (3) and wavelength-shift of the two peaks.

In conclusion, an ultrahigh birefringence PCF with an elliptical core was fabricated and analyzed experimentally and theoretically. Birefringence as high as 1.1×10^{-2} at the wavelength of 1550 nm was obtained experimentally. To our knowledge, this is the highest birefringence reported for PM–PCFs. The core is Ge-doped and FBG written on the PCF exhibit a large peak separation over 12 nm. Pressure and temperature responses were investigated using FBG inscribed in the PCF demonstrating its capability to measure pressure and temperature simultaneously.

This work is supported by The Hong Kong Polytechnic University under Grant No. 4-ZZE4.

References

1. T. A. Birks, J. C. Knight, and P. S. Russell, Opt. Lett. **22**, 961 (1997).
2. P. St. J. Russell, J. Lightwave Technol. **24**, 4729 (2006).
3. A. Ortigosa-Blanch, J. Knight, and W. Wadsworth, Opt. Lett. **25**, 1325 (2000).
4. D. Chen and L. Shen, IEEE Photon. Technol. Lett. **19**, 185 (2007).
5. T. P. Hansen, J. Broeng, S. E. B. Libori, E. Knudsen, A. Bjarklev, J. R. Jensen, and H. Simonsen, IEEE Photon. Technol. Lett. **13**, 588 (2001).
6. H. Y. Fu, H. Y. Tam, L.-Y. Shao, X. Dong, P. K. A. Wai, C. Lu, and S. K. Khijwania, Appl. Opt. **47**, 2835 (2008).
7. O. Frazao and C. Jesus, IEEE Photon. Technol. Lett. **21**, 1277 (2009).
8. B. Guan, D. Chen, and Y. Zhang, IEEE Photon. Technol. Lett. **20**, 1980 (2008).
9. T. Tenderenda, K. Skorupski, M. Makara, G. Statkiewicz-Barabach, P. Mergo, P. Marc, L. R. Jaroszewicz, and T. Nasilowski, Opt. Express **20**, 26996 (2012).
10. A. Michie, J. Canning, K. Lyytikäinen, M. Aslund, and J. Digweed, Opt. Express **12**, 5160 (2004).
11. A. Ortigosa-Blanch, IEEE Photon. Technol. Lett. **16**, 1667 (2004).
12. M. Szpulak, T. Martynkien, and W. Urbanczyk, in *International Conference on Transparent Optical Networks* (IEEE, 2006), pp. 174–177.
13. F. Beltrán-Mejía, G. Chesini, E. Silvestre, A. K. George, J. C. Knight, and C. M. B. Cordeiro, Opt. Lett. **35**, 544 (2010).
14. X. Chen, M.-J. Li, N. Venkataraman, M. Gallagher, W. Wood, A. Crowley, J. Carberry, L. Zenteno, and K. Koch, Opt. Express **12**, 3888 (2004).
15. M. S. Alam, K. Saitoh, and M. Koshiba, Opt. Lett. **30**, 824 (2005).
16. M. L. V. Tse, K. M. Chung, L. Dong, B. K. Thomas, L. B. Fu, K. C. D. Cheng, C. Lu, and H. Y. Tam, Opt. Express **18**, 17373 (2010).
17. Z. Liu, M.-L. V. Tse, C. Wu, D. Chen, C. Lu, and H.-Y. Tam, Opt. Express **20**, 21749 (2012).
18. M. L. V. Tse, H. Y. Tam, L. B. Fu, B. K. Thomas, L. Dong, C. Lu, and P. K. A. Wai, IEEE Photon. Technol. Lett. **21**, 164 (2009).
19. F. C. Fávero, S. M. M. Quintero, C. Martelli, A. M. B. Braga, V. V. Silva, I. C. S. Carvalho, R. W. A. Llerena, and L. C. G. Valente, Sensors **10**, 9698 (2010).